Final State Photon Radiation from Quarks and Comparison with QCD Models

A. Perrotta

Dipartimento di Fisica, Università di Bologna, and

INFN, Sezione di Bologna, Italy

May 25, 1994

Abstract

A photon selection algorithm is applied to neutral showers in the hadronic decays of the Z^0. Its performances have been studied relying completely on real data reference samples, in order to avoid distortions coming from the uncertainties in the MonteCarlo modelization, The rate of Final State photon Radiation from quarks is extracted from DELPHI 1992 data using this algorithm. The experimental rate is compared with the predictions of two MonteCarlo programs, GNJETS and EEPRAD, based on $\mathcal{O}(\alpha\alpha_s)$ ME calculations. The relative ratio of 1, 2 and 3 jets plus γ events is in good agreement with the predictions, once the $\alpha_s^{(1)}$ parameter is properly choosen. The overall number of events with final state radiation photons is also found in agreement with ME predictions. Nevertheless, this number lies slightly below the theoretical expectation, confirming a common trend seen also in the analysis of the other LEP experiments.

1 Introduction

The study of Final State photon Radiation (FSR) from quarks is comparatively easier at LEP with respect to previous e^+e^- colliders working at lower energies, thanks to the Z^0 resonance shape that strongly suppresses the contribution of Initial State Radiation (ISR) [1].
Quarks and gluons arising from the QCD cascade suffer further interactions before attaining the detectable hadronic final state. Only the photon can reach the detector in the same condition as it was emitted: it is a good witness of what happens in the early perturbative stages of the evolution of an hadronic event.
Selecting FSR photons amongs other types of photons and background showers that can be found in the hadronic Z^0 decays is the main experimental task in making such an analysis.
ISR is strongly suppressed at large angles from the beams. Hadronization remnants tend to lie inside the hadronic jets, unless they are too soft, while FSR photons are usually scattered at larger angles. Then, qualitatively, one can enrich the FSR sample looking for isolated and energetic neutral electromagnetic showers at large polar angles. Some amount of background ultimately remains in that sample; such an amount must be carefully evaluated in order to estimate the real FSR rate in hadronic events at LEP.
A FSR analysis in DELPHI was already performed based on 1989 and 1990 data, and the results have been published in [2]. In the present paper a new selection method to extract the number of FSR photons from a sample of isolated shower in hadronic Z^0 decays is applied to 1992 DELPHI data.

2 FSR in $\mathcal{O}(\alpha\alpha_s)$ calculations

Although all Parton Showers (PS) programs in use in high energy e^+e^- physics include FSR, it is supposed that hard processes like γ radiation in the early stage of the hadronic cascade could be conveniently explained in term of Matrix Element (ME) calculations [3].
Some of the diagrams that contribute to the $\mathcal{O}(\alpha\alpha_s)$ calculations are drawn in Fig. 1. Several MonteCarlo (MC) implementations of these calculations are available.In this note, two of them will be taken into account: GNJETS [4], based on an analytical calculation originally made by Kramer and Lampe [5], and EEPRAD [6], based on a calculation by Glover and Stirlig . Details of the two MC and on the ME calculations can be found in the references quoted. Only a few points will be underlined in the following.
Given a jet resolution parameter y_{cut}, the ME's calculate the partial ratios in 1, 2 or 3 jets according to

$$\frac{\Gamma\,(Z\,\rightarrow\,\gamma\;+\;n\,jets)}{\Gamma\,(Z\,\rightarrow\,hadrons)}\;=\;\mathcal{N}g_n(y) \tag{1}$$

where

$$\mathcal{N} = \frac{\frac{8}{9}c_u+\frac{1}{3}c_d}{2c_u+3c_d}\frac{\alpha_{em}}{2\pi}\left(1+\frac{\alpha_s}{\pi}+1.41\left(\frac{\alpha_s}{\pi}\right)^2\right)^{-1} \tag{2}$$

$$c_f = v_f^2+a_f^2 \qquad f=u,d \tag{3}$$

The vector and axial couplings of the quarks to the Z^0 are given by

$$v_f = 2I_{3,f}-4Q_f\sin^2\Theta_W \tag{4}$$

$$a_f = 2I_{3,f} \tag{5}$$

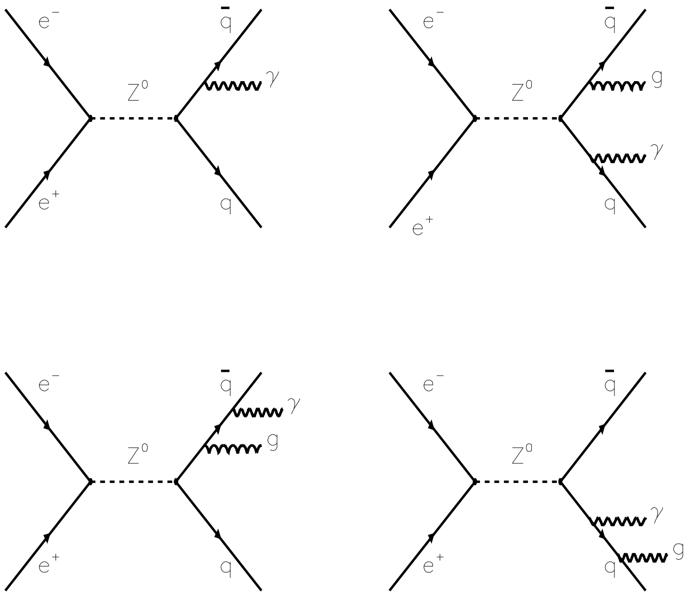

Figure 1: *Some of the Feynmann graphs at order $(\alpha\alpha_s)$ that contribute to the cross section of the process $e^+e^- \to q\bar{q}\gamma(g)$*

where $I_{3,f}$ is the third component of the weak isospin, Q_f the electric charge of the quark and Θ_W is the Weinberg electroweak mixing angle.
The normalization factor in the FSR cross sections is proportional to $8c_u + 3c_d$ because the photon radiation depends on the square of the quark electric charge. Then the *up* type quarks contribution to FSR is enhanced by a factor of 4 when compared to the contribution given to the overall hadronic cross section.
The results for $g_n(y)$ have been obtained analytically. They contain a term which does not depend on the strong coupling constant and one which is proportional to it:

$$\begin{aligned} g_1(y) &= g_1^{(0)}(y) + \frac{\alpha_s^{(1)}}{2\pi} g_1^{(1)}(y) \\ g_2(y) &= g_2^{(0)}(y) + \frac{\alpha_s^{(1)}}{2\pi} g_2^{(1)}(y) \\ g_3(y) &= \frac{\alpha_s^{(1)}}{2\pi} g_3^{(1)}(y)\,. \end{aligned} \tag{6}$$

$\alpha_s^{(1)}$ is not the same as the one obtained by LEP experiments at the M_Z^2 scale and that enters in the expression for the normalization factor in equation 2. In fact, the approximations deriving from

stopping the calculation to the first order in α_s can be taken into account by choosing a lower scale for the strong coupling constant.
The resolution parameter y is here defined in term of the Durham algorithm [7] with recombination scheme "E":

$$y_{ij} = \frac{2\min\{E_i^2, E_j^2\}(1-\cos\theta_{ij})}{E_{vis}^2} \tag{7}$$

$$p_{ij}^{\mu} = p_i^{\mu} + p_j^{\mu} \, . \tag{8}$$

$\mathcal{O}(\alpha\alpha_s)$ calculations contain poles in the region where qg are collinear (QCD poles), in the region where $q\gamma$ are collinear and for very low energetic photons. Cuts on the photon energy and on the photon isolation with respect to the other partons must be included during the generation. Nevertheless, a completely isolated photon is not IR finite at the order $(\alpha\alpha_s)$, because the divergences arising from γg collinearities act as a counterterm that cancels other kind of divergences. The method used to violate perfect isolation represents the main difference between the two programs. GNJETS requires isolation with respect to the pair qg, not with respect to the gluon alone, while EEPRAD admits soft gluons, regulated by a cut-off parameter, inside the photon isolation cone.
In the implementation of the two MC used in the present analysis the photon isolation is defined in term of the lowest angular distance admitted with respect to the closer parton in the event, θ_{iso}. On the experimental side of the analysis, an isolation cone of 20^o will be used. Then the dependence of the MC's to the cuts on generation has been studied generating events with isolation angle of 5^o, 10^o, 15^o and 20^o .
Another source of error for the MC predictions is found in the unphysical parameter y_0 that settles the singularities arising from collinear quarks and gluons and from soft gluons. y_0 has been moved from 10^{-4} to 10^{-6} in GNJETS, as suggested in [3], and from $y_{cut}/1000$ to $y_{cut}/50$ in EEPRAD.
In Fig. 2 one can see the ratios of EEPRAD to GNJETS cross sections for 1, 2 and 3 jets plus γ (the absolute cross sections will be shown later in comparison with DELPHI data) as a function of y_{cut}. The widths of the distributions reflect the MC statistics used when running the two programs (which is slightly lower in GNJETS) and the response to the variation of the generation parameters (which looks larger in GNJETS than in EEPRAD).

2.1 How to get the free parameters from the comparison of ME calculation with the data

From equations 1 and 6 one can see that the ME calculations, and their MC implementations, depend on two free parameters: $\alpha_s^{(1)}$ and $\mathcal{N}$.
$\alpha_s^{(1)}$ can be derived independently looking, for instance, at the relative ratios of 3 jets events over $2+3$ jet events:

$$\mathcal{R}_3(y_{cut}) = \frac{\sigma_{3\,jets+\gamma}}{\sigma_{2\,jets+\gamma} + \sigma_{3\,jets+\gamma}} \, . \tag{9}$$

The $\mathcal{R}_3$ extracted from the data can be compared with the $\mathcal{R}_3$ predicted by the MC using different values of $\alpha_s^{(1)}$.
Once $\alpha_s^{(1)}$ is known, that value can be used to compute the total cross section. Comparing the total cross sections for $q\bar{q}\gamma$ events in the data and in the ME calculations provides the normalization factor $\mathcal{N}$, that is the combination $8c_u + 3c_d$. Such a combination gives the individual c_u and c_d once intersected with the combination $2c_u + 3c_d$ extracted from the total hadronic width of the Z^0 [8]:

$$\Gamma_{had} = \frac{3M_Z^3 G_\mu}{24\pi\sqrt{2}}\left[1 + \frac{\alpha_s}{\pi} + 1.4\left(\frac{\alpha_s}{\pi}\right)^2\right](2c_u + 3c_d) \, . \tag{10}$$

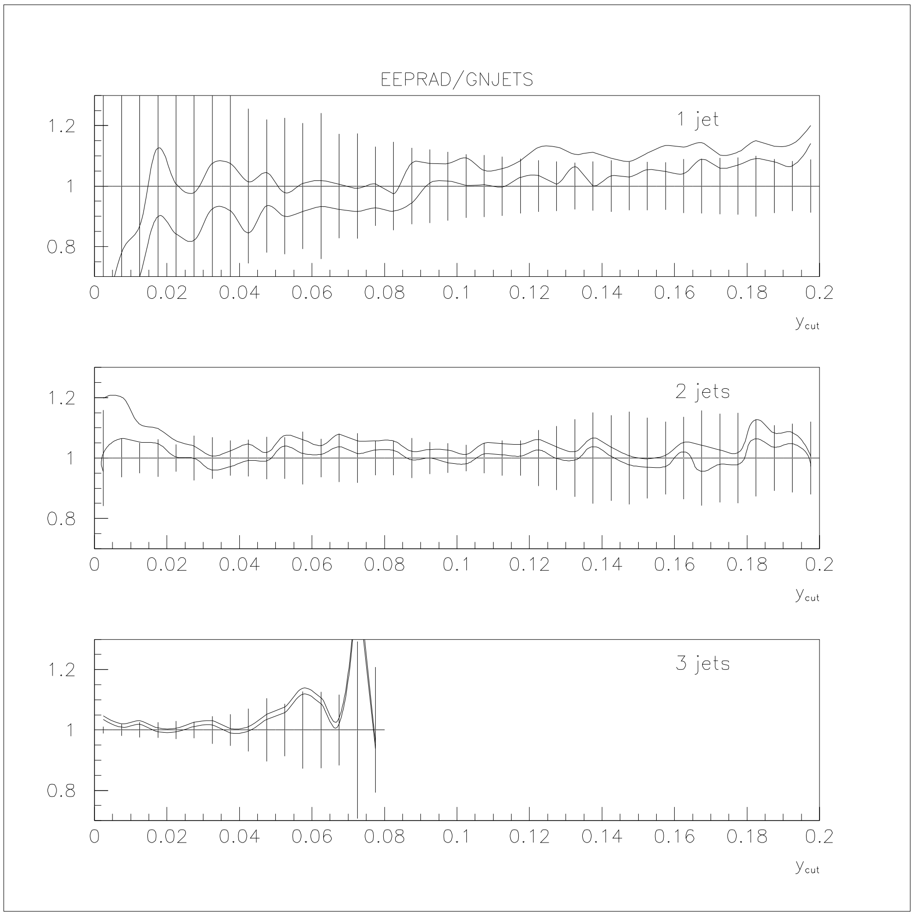

Figure 2: *Ratio between the jet rates foreseen by EEPRAD and those foreseen by GNJETS* ($\alpha_s^{(1)} =$ 0.17 *in both cases)*

Using $G_\mu = 1.16639 \cdot 10^{-5}$ GeV^{-2} [9], $\alpha_s^{(2)} = (0.123 \pm .007)$ [10], $M_Z = (91.187 \pm 0.009)$ GeV and $\Gamma_{had} = (1.725 \pm 0.012)$ GeV [11], one has

$$2c_u + 3c_d = 6.66 \pm 0.05\,. \tag{11}$$

3 Neutral showers in the HPC

To suppress the background coming from ISR, the analysis is restricted to the neutral showers fully contained in the DELPHI barrel electromagnetic calorimeter HPC [12, 13]. Only events collected during 1992 runs are used. They have been processed using version 92C of the DELPHI standard analysis program DELANA [14].
The adjustments of the HPC data applied during the analysis are discussed in this section.

3.1 Non linearity in the HPC response

Several causes may determine the non linearity of the response in a real-life calorimeter. For the HPC, deviations from proportionality of the shower energy with respect to the charge collected in the read-out pads can arise from:

- material in front of the HPC;
- incomplete containement of the shower in the 17.3 radiation lengths of the calorimeter;
- gas saturation;
- non linearity in the electronics;
- pedestals subtraction.

A correction to the energy of the neutral electromagnetic showers written in the Data Summary Tapes (DST) [15] created using DELANA 92C is suggested in [16]:

$$E \to E' = E \cdot \frac{1 - 0.44/45.6^{\,0.18}}{1 - 0.44/E^{\,0.18}} \tag{12}$$

$$E' \to E'' = E' \cdot \left[1 - 0.55 \cdot \exp\left(-\frac{E'}{0.36}\right) + 0.056 \cdot \left(1 - \frac{E'}{45.6}\right)\right]^{-1} . \tag{13}$$

The effect of the two corrections on the energy of simulated photon showers passed through a full DELPHI simulation with DELSIM [17] can be seen in Fig. 3, where the measured energy is compared to the generated one.
Checking the effect of non-linearity corrections on real photons themselves is not so easy, because it is hard to estimate the photon energy independently from any calorimetric information. The agreement between data and simulation may be tested comparing simulated electrons and Compton ones. The momenta of Compton electrons can be derived directly from the cinematics of the event or from the tracking informations [18].
The energy correction applied to neutral showers needs not to be the same as for charged showers. In effect a stronger correction would be needed (e.g. using only equation 12) to take further into account the possibility of electron bremsstrahlung in the material in front of the HPC. Nevertheless, considering the largest deviations between the simulated electron energies and the real ones in the momentum range $|\vec{P}| > 5$ GeV, one gets:

$$E_{MC} - E_{data} = (0\,^{+200}_{-65})\, MeV\,. \tag{14}$$

Such a variation will be taken into account when evaluating the systematic uncertainties of the results.

3.2 Fixing to the isolation criteria for high energy showers

It is well known that when soft electrons or positrons from the electromagnetic shower curl in the drift channels of the HPC they can generate fake HPC clusters in the neighbouring of a real shower. These clusters can be combined by the HPC pattern recognition algorithm [19] with other fake clusters (of the same origin, or coming from α decays in the converter material, or any other kind of noise) to generate a fake neutral electromagnetic shower. If this shower falls inside the isolation cone, the photon may be discarded by the isolation criteria (Table 1).
The effect of curling electrons is not fully included in the HPC simulation, where they are stopped in the vicinity of the parent shower in order to avoid that the computation time blows up. As a result, more isolated showers are found in the simulation than in the real data, even if the initial event topology is the same.

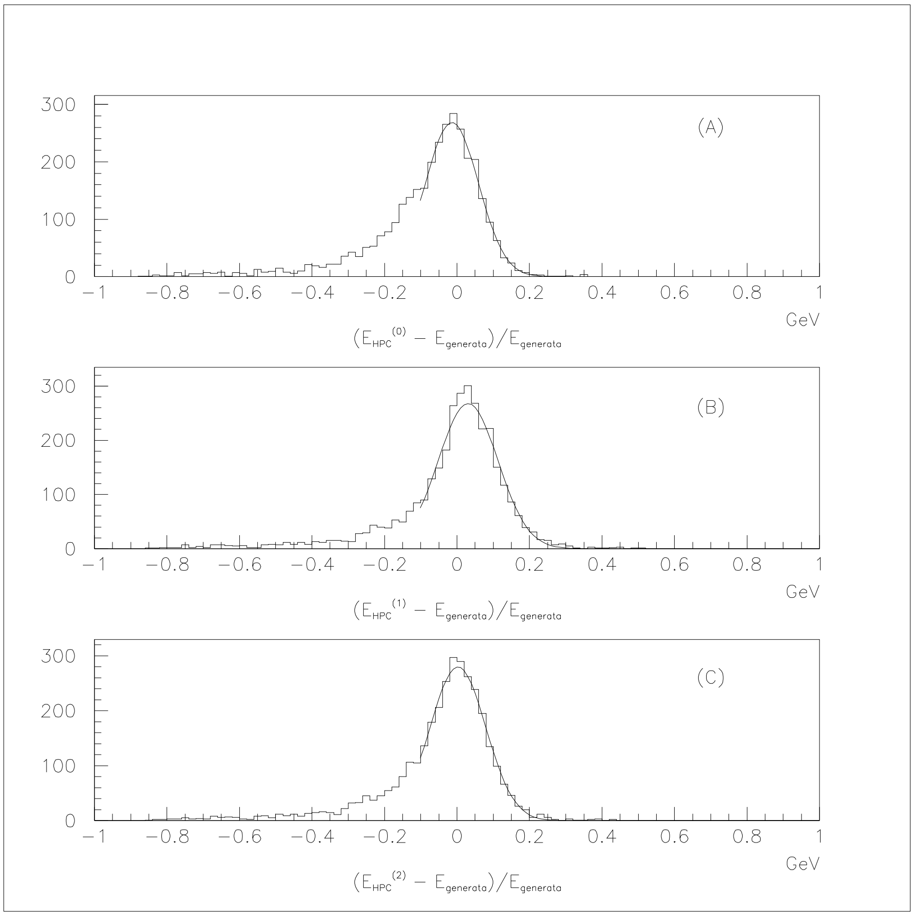

Figure 3: *Photons in the HPC simulation: (A) difference between the energy written in the DST and the generated energy; (B) the same when the first correction is applied; (C) the same when also the second correction is applied.*

The probability of having curling electrons increases for high energy showers. Then one expects that the effect will become more and more important as the shower energy increases.
Since the fake showers have necessarily no associated charged tracks, one can compare between data and MC the number of showers having only charged particles in the isolation cone and the number of showers having only neutral showers inside the isolation cone.
To do that, the following quantities have been defined on data and MC samples:

$$\mathcal{R}^{\pm}(E) = \frac{N(E^{\pm}_{iso} < 0.5\, GeV)}{N(E^{\pm}_{iso} < 3\, GeV)} \tag{15}$$

$$\mathcal{R}^{0}(E) = \frac{N(E^{0}_{iso} < 0.5\, GeV)}{N(E^{0}_{iso} < 3\, GeV)} \tag{16}$$

where the first ratio is taken between showers having only charged particles in the isolation cone and the second one is taken between showers having only neutral particles in the isolation cone.
Fig. 4 reports the ratios $\mathcal{R}^{\pm}_{MC}/\mathcal{R}^{\pm}_{data}$ and $\mathcal{R}^{0}_{MC}/\mathcal{R}^{0}_{data}$. One can see that the first ratio is compatible with 1 and independent on the energy, as expected. The second ratio, instead, grows with the shower energy.
In order to have a MC that behaves similarly to the data, all the MC distributions at the detector

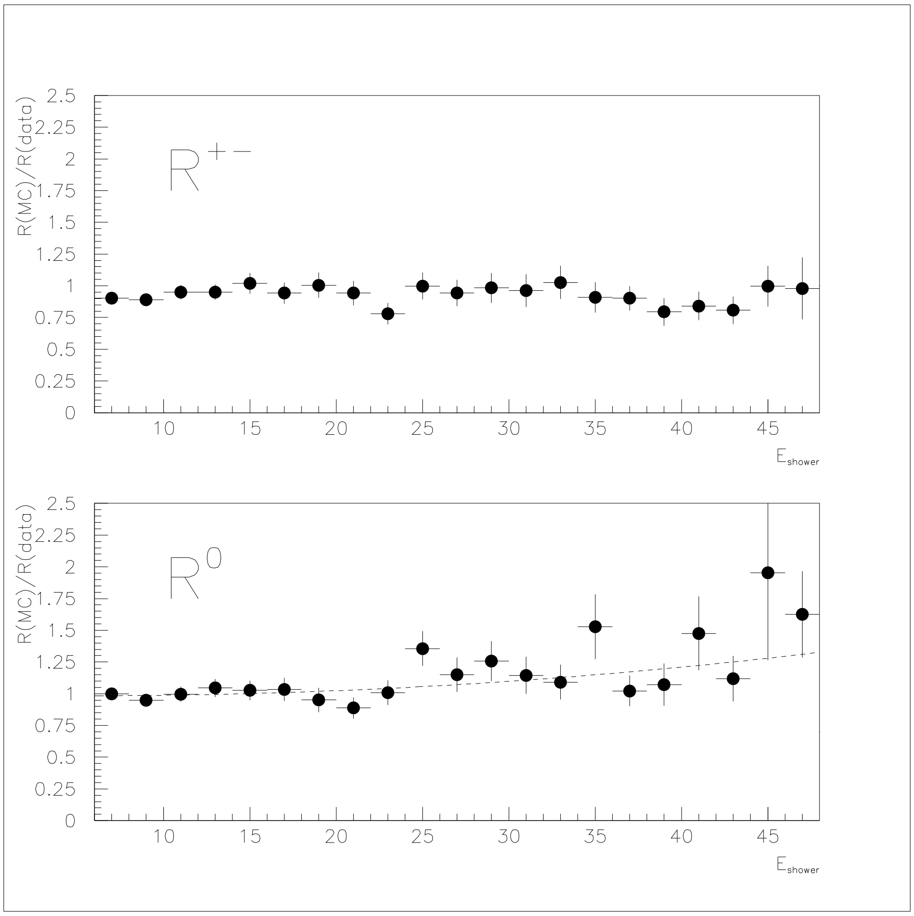

Figure 4: *Ratios $\mathcal{R}^{\pm}_{MC}/\mathcal{R}^{\pm}_{data}$ e $\mathcal{R}^{0}_{MC}/\mathcal{R}^{0}_{data}$, as defined in the text. On the second one is superimposed the function used to fix the high energy shower losses*

level have been weighted with a correction factor depending on the energy of the shower:

$$CORR(E) = \frac{\mathcal{R}^{0}_{data}}{\mathcal{R}^{0}_{MC}}\,. \tag{17}$$

A second order polynomial has been adapted to the second histogram in Fig. 4 to parametrize the effect. The result for the correction factor that is used in the present analysis is:

$$[CORR(E)]^{-1} = 0.99 - 0.21 \cdot 10^{-2} E + 1.9 \cdot 10^{-4} E^2\,, \tag{18}$$

with E in GeV. The error also depends on the shower energy:

$$\Delta\left([CORR(E)]^{-1}\right) = |\,0.03 - 0.14 \cdot 10^{-2} E + 0.8 \cdot 10^{-4} E^2\,|\,. \tag{19}$$

4 Determination of FSR rate in 92C data

4.1 Selection of the samples of showers

The method used to determine the FSR rate directly from the real data has been described in [20]. It turns out to be almost fully independent on the event and detector simulations, overcoming the

	"FSR"	"γ"	"Background"
Event selection	hadronics	leptonics	hadronics
E_γ^{min}	5.5 GeV	5.5 GeV	5.5 GeV
θ_γ^{min}	45^o	45^o	45^o
Isolation	$E < 0.5$ GeV in 20^o	$12.5^o < \theta_{iso} < 170^o$	$0.5 < E^{char} < 3$ GeV $E^{neutral} < 0.5$ GeV in 20^o
N. of showers	1405	829	1031
Estimated FSR + ISR content	*to be determined*	$\simeq 98\%$	$\simeq 11\%$

Table 1: *Selection criteria for the signal and reference samples used in the analysis*

uncertainties from the potentially incorrect treatment of particles emitted far from the jet core in the event generators and from the simulation of the lateral spread of the electromagnetic shower in the calorimeter.

To summarize the method, three samples of showers are extracted from the real data themselves. One of them contains FSR photons, one is used as a reference sample for the photons and one as a reference sample for the typical background to FSR still present in the first sample. The selections of hadronic and leptonic events follow the ones adopted in several DELPHI analyses, based on particle multiplicity and visible energy [11]. The whole analysis is based on $599,064$ selected hadronic events.

The selection criteria for the three different types of showers are summarized in Table 1. The isolation of the two samples of showers extracted from the selected hadronic events are defined in term of a maximum amount of energy allowed inside the isolation cone of 20^o. The background sample has been choosen among the partially isolated showers. The partial isolation criterion admits only charged particles inside the isolation cone. This choice of the background reference showers has been optimized by looking at the agreement both in the energy and in the shower shape variables spectra, between the background reference sample and the "true" background showers to the fully isolated FSR photons in the simulation.

4.2 Preliminar cuts on the showers

The numbers of showers entering in Table 1 include the cuts to avoid the gaps in ϕ between the TPC modules and and the gaps in ϕ and θ between the HPC modules, i.e. the showers are not accepted if:

- ϕ is whithin $\pm 2^o$ around the center of the 6 TPC dead zones in ϕ;

- ϕ is whithin $\pm 1^o$ around the center of the 24 HPC dead zones in ϕ;
- $|\theta - 90^o|$ is in the intervals $[0, 1.8^o]$, $[20^o, 23.5^o]$ and $[37.5^o, 40^o]$.

The widths of the forbidden regions have been choosen looking directly in the data for distortions in the shower energy or in the shower shape distributions.
When the data are compared with ME calculations, they must be extrapolated to the whole solid angle. The extrapolation factor depending on ϕ is obtained from the isotropy in the ϕ distributions:

$$\phi_{norm} = 1.25 \tag{20}$$

When computing the extrapolation factor that depends on θ, one must take into account the behaviour of the theta distribution of the FSR photons. One can expect a distribution like [21]

$$\frac{d\sigma}{d\theta} \propto 1 + A\cos^2\theta\,, \tag{21}$$

with $0 < A < 1$. Fitting the shape of the distribution of FSR photons generated with JETSET PS [22] one gets

$$A = 0.412 \pm 0.060\,, \tag{22}$$

from which

$$\theta_{norm} = 1.820 \pm 0.014\,. \tag{23}$$

4.3 Noise rejection

The numbers in Table 1 include also the cuts for noise rejection:

- at least 4 HPC layers hit;
- the shower must start not later than in the 5^{th} HPC layer;
- $E_{MAX}/E_{TOT} < 0.7$;
- $|\theta_{shower} - \theta_{vertex}| < 20^o$;
- $|\phi_{shower} - \phi_{vertex}| < 30^o$;

Here the subscripts 'shower' and 'vertex' indicate respectively the angles computed from the shower direction and from the extrapolation of the shower starting point to the interaction vertex. MAX refers to the HPC layer with the maximum deposited energy.
A detailed discussion of these cuts is presented in [20]. They are supposed to completely discard the residual noise showers in the HPC (that could arise, for instance, from α decays in the HPC converters). They represent also a sort of request of electromagneticity for the shower.
Photons are almost transparent to these cuts:

$$\varepsilon_\gamma^{noise} = 0.997 \pm 0.002\,, \tag{24}$$

while background showers are purged of the ones that do not look electromagnetic:

$$\varepsilon_{bckg}^{noise} = 0.719 \pm 0.035\,. \tag{25}$$

These two numbers are derived applying the above cuts to simulated showers, since the longitudinal shower development is sufficiently well described in the simulation.

4.4 Variables used to discriminate and their efficiencies

The main source of background to FSR photons resides in the hadronization remnants, mainly π^0. π^0's decay in two photons that can be separated of such a small angle that their electromagnetic showers overlap in the HPC and are seen as a unique broader shower. A typical way to select single photons is then to use the lateral shape of the shower in the calorimeter.
Two variables have been defined to parametrize the lateral shower shape. They exploit the HPC spatial resolution in testing whether the shower points to the primary vertex, characterizing also some of the non prompt photons coming from bremsstrahlung or particle decays.
Thes two variables are defined as

$$A1 = \frac{1}{E_{sum}} \cdot \sum_{i=1}^{N_{cl}} \left((\vec{r}_i, \vec{r}_{bar}) \cdot E_i \right) \tag{26}$$

$$A2 = \frac{1}{E_{sum}} \cdot \sum_{i=1}^{N_{cl}} \left((\vec{r}_i, \vec{r}_{in}) \cdot E_i \right) \tag{27}$$

where the sum is performed over all HPC clusters and

$$E_{sum} = \sum_{i=1}^{N_{cl}} E_i \,. \tag{28}$$

$(\vec{r}_i, \vec{r}_{bar})$ is the angle between the direction from the primary vertex to the cluster maximum and the direction from the primary vertex to the baricenter of the shower; $(\vec{r}_i, \vec{r}_{in})$ is similar but the second direction is taken to the starting point of the shower. All the angles are measured in degrees. Comparing the photon data sample and the background data sample one can see in Fig. 5 that $\max\{A1, A2\}$ can discriminate between the two classes of showers.
By using the two reference sample it is possible to compute the efficiency of a cut in $\max\{A1, A2\}$. The formula used can be found in [20]. Fig. 6 shows the efficiencies for photons and for the typical background with a cut $\max\{A1, A2\} < 0.75$, computed in eight different energy bins.
The overall average value of the two efficiencies in all $E > 5.5$ GeV showers (this is correct for photons, whose efficiency does not seem to depend on E, but it may be not too meaningful for the background), including also the effects of the noise rejection cut, is:

$$\begin{aligned} \varepsilon_\gamma &\simeq 90\% \\ \varepsilon_{bckg} &\simeq 39\% \quad . \end{aligned}$$

In the following, all the efficiencies will be entered correctly in the calculations, separately in each energy bin.

4.5 FSR rate in the isolated shower sample

To determine the photon content in the isolated shower sample one has, before and after having applied the cuts on $\max\{A1, A2\}$:

$$N_\gamma + N_\pi = N \tag{29}$$

$$\varepsilon_\gamma N_\gamma + \varepsilon_\pi N_\pi = N_1 \,. \tag{30}$$

where N_γ and N_π are respectively the numbers of photon and background showers in the sample, ε_γ and ε_π their efficencies for the given cut, N and N_1 the overall number of showers in the sample before and after the cut. N_γ is the number of FSR (+ISR) showers that one wants to determine.

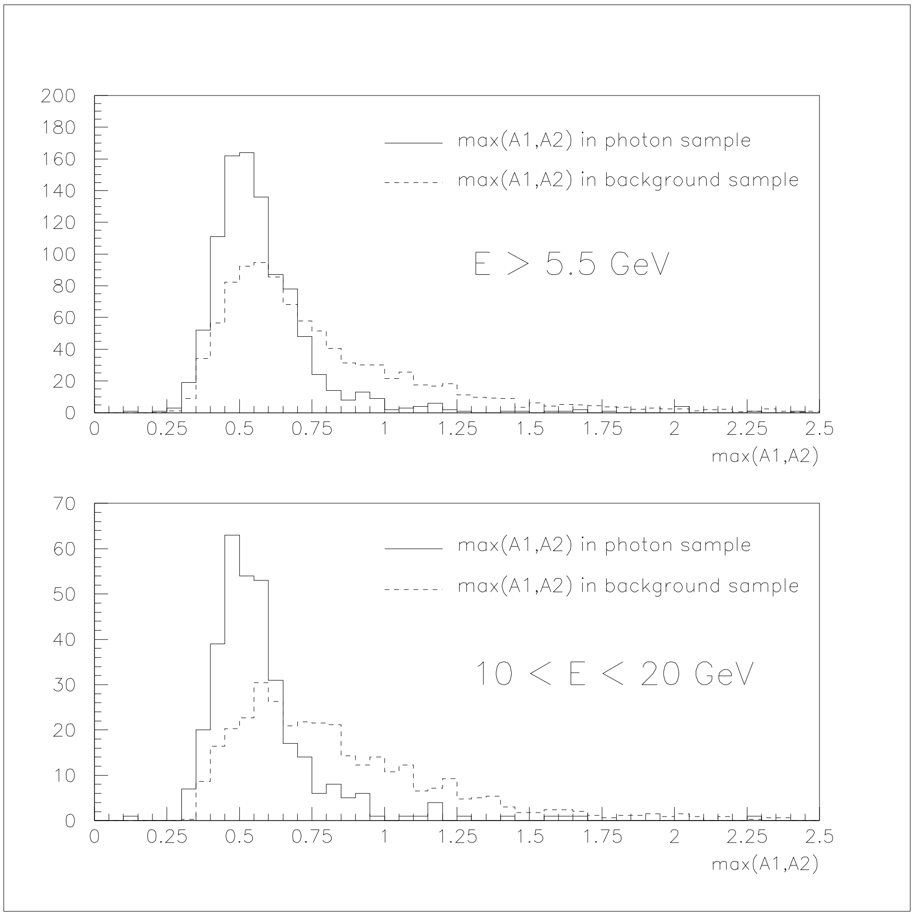

Figure 5: $\max\{A1, A2\}$ *distributions in the photon and background reference samples. Above, all showers with* $E > 5.5$ *GeV are considered, while below only the showers with* $10 < E < 20$ *GeV are shown, where the algorithm permits a more efficient separation of the two samples. In the background reference sample is still included a content of* $\simeq 11\%$ *of true FSR or ISR photons.*

Solving one has:

$$n_\pi = \frac{N_\pi}{N} = \frac{1}{\varepsilon_\gamma - \varepsilon_\pi}\left(\varepsilon_\gamma - \frac{N_1}{N}\right) \tag{31}$$

$$n_\gamma = \frac{N_\gamma}{N} = 1 - n_\pi \tag{32}$$

$$\Delta n_\pi = \frac{1}{\varepsilon_\gamma - \varepsilon_\pi}\Delta\left(\frac{N_1}{N}\right) \oplus \left|\frac{\varepsilon_\gamma - n_1}{(\varepsilon_\gamma - \varepsilon_\pi)^2}\right|\Delta\varepsilon_\pi \oplus \left|\frac{n_1 - \varepsilon_\pi}{(\varepsilon_\gamma - \varepsilon_\pi)^2}\right|\Delta\varepsilon_\gamma \tag{33}$$

$$\Delta n_\gamma = \Delta n_\pi \ . \tag{34}$$

In the analysis sample, the number of photons present before applying the cuts is determined bin per bin using equation 32. All the contents of the eight energy bins are then summed together. The number of photons obtained in that way must be subtracted of ISR and corrected for the photons coming from the few residuals $e^+e^- \to \tau^+\tau^-$ events in the hadronic sample. The ISR content is determined using JETSET PS predictions. The correction for $\tau^+\tau^-$ events comes from the MC and from the knowledge of the relative ratios in Z^0 decays.

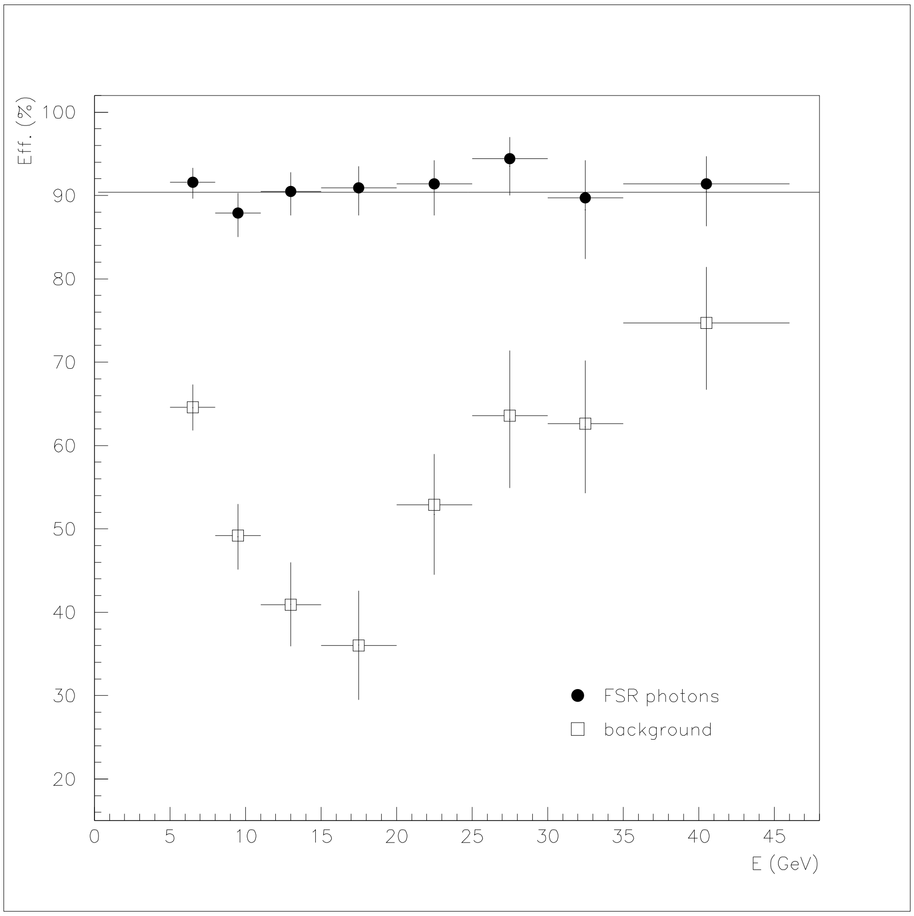

Figure 6: *Efficiencies for FSR photons and for background showers to the cut* $\max\{A1, A2\} < 0.75$, *as a function of the shower energy*

Table 2 shows the number of FSR photons in the isolated shower sample once a further cut on $y_{ij} > y_{cut}$ is applied. One can see that the FSR represent something more than the 60% of the whole sample of isolated showers. The errors shown in the table are the statistical one, the error due to the selection (equation 34), the errors due to the subtraction of ISR and taking into account the $\tau^+\tau^-$ content, the error coming from the uncertainty on the energy of the showers (equation 14).

5 Comparison with JETSET PS

The JETSET PS [22] MC version 7.3, independently tuned to many distributions extracted from the hadronic events in DELPHI [23] and used to generate the simulation data, is compared to the experimental FSR ratios of 1, 2, 3 jets + γ. The results of the comparison can be seen in Fig. 7 as a function of y_{cut}. The FSR rates have been normalized to the total number of hadronic events corresponding to the selected ones.
The errors in the data include all the items tabulated in Table 2. The errors in the MC come from statistics and from the uncertainty on the factor fixing the reduced efficiency in real data for isolation cuts at higher shower energies (equation 19), added in quadrature.

y_{cut}	All showers	Nr. FSR	Δ(stat)	Δ(comp)	Δ(ISR)	$\Delta(\tau)$	$\Delta(\Delta E)$
0.01	911	560	24	47	5	2	15
0.02	712	450	21	40	3	1	4
0.03	580	359	19	39	2	1	2
0.04	506	293	17	37	2	1	2
0.05	461	256	16	37	2	1	2
0.06	428	241	16	36	2	1	2
0.07	397	220	15	34	2	1	3
0.08	382	213	15	36	2	1	3
0.09	371	204	14	36	2	1	3
0.10	371	216	15	35	2	1	3
0.15	361	218	15	35	2	1	3
0.20	358	223	15	36	2	1	2

Table 2: *Number of final state radiation photons in the 1992 DELPHI data after angular cuts and isolation cuts with respect to the other particles, as a function of the γ jet isolation parameter y_{cut}*

6 Conversion factor (parton level) / (detector level)

The events generated with ME MC's consist of partons (quarks, gluons and photons). Computing them at the order $(\alpha\alpha_s)$, one ends with at least three $(q\bar{q}\gamma)$ and at most four $(q\bar{q}g\gamma)$ partons. ISR is not included in the generators.
It is clear that isolation criteria, recombination algorithm, etc. act somewhat differently depending on the multiplicity of the state to which they are applied. Fig. 8 (A) shows the total multiplicity seen in the hadronic events with an isolated shower, in the data and in JETSET + DELSIM simulation.
Let us define three levels for the events.

- Parton level: the one assumed by fundamental partons at the end of the perturbative phase, before fragmentation.
- Hadron level: the whole of final state particles at the end of the evolution.
- Detector level: all tracks and showers reconstruted in the detector.

ME's compute parton level cross sections, while from the data one measures detector level cross sections. A convertion factor is therefore needed in order to connect the two levels:

$$c = c_1 \cdot c_2 \,, \tag{35}$$

where $c_1 = \sigma_{parton}/\sigma_{hadron}$ includes corrections due to the modelization of the hadronic shower and $c_2 = \sigma_{hadron}/\sigma_{detector}$ includes detector effects.
c_2 is easily obtained comparing simulated events at the hadron level and after passed through a complete detector simulation.
For c_1 several possibilities exist. In any case such a factor will depend significantly on the parton multiplicity and on the parton jet structure. At the usual parton level of JETSET PS, get at the

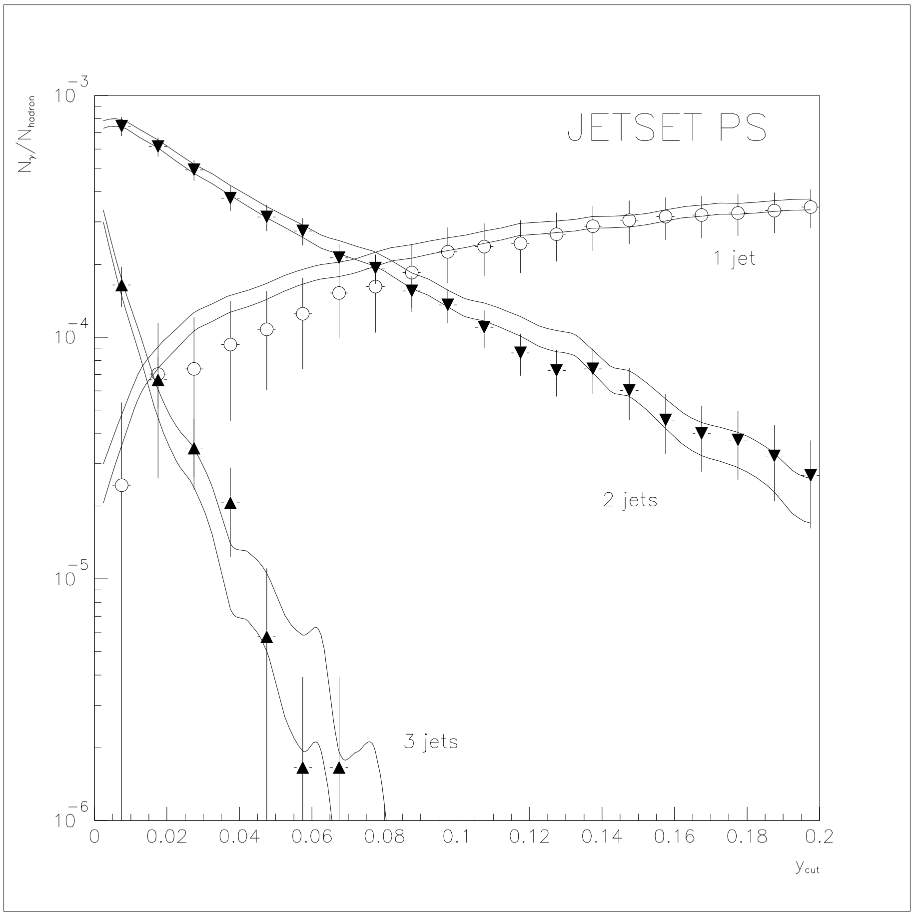

Figure 7: *Comparison of* 1, 2 *and* 3 *jets plus* γ *events between 1992 DELPHI data (points with errors) and JETSET PS (strips representing the mean value plus and minus* 1σ*). In all cases the associated errors combine the statistical and the systematic ones. Points at different* y_{cut} *are strictly correlated.*

end of the perturbative cascade, one has a parton multiplicity (see Fig. 8 (B)) which is often more than twice the ME multiplicity it should simulate.
A more correct way of getting the factor c_1 consists in fragmenting directly the final states given by the ME's. The fragmentation can be performed using the routines of the JETSET package, already tuned to LEP data. Such a method of computing c_1 is nevertheless not exempt from uncertainties. In fact the parton level generated by ME MC programs does not span the whole phase space but it is restricted to particular regions by cuts applied during the generation of the event. To be as much independent as possible of the generation cuts, c_1 has been derived comparing the partonic final state given by GNJETS, spanning over the same range of cuts used to study the sensitivity of the MC's, with the hadronic state obtained fragmenting the same parton level. The dependence on the jet structure has been taken into account ranging $\alpha_s^{(1)}$ from 0.14 to 0.20 during generation. The c_1 factors computed according to the procedure outlined above for 1, 2 and 3 jets + γ events are shown in Fig. 9. For comparison (but they are not used in the analysis) one can see superimposed the corresponding factors derived from the parton level of JETSET PS and from an artificial few-parton level of JETSET obtained by stopping the evolution after the radiation of the first gluon.

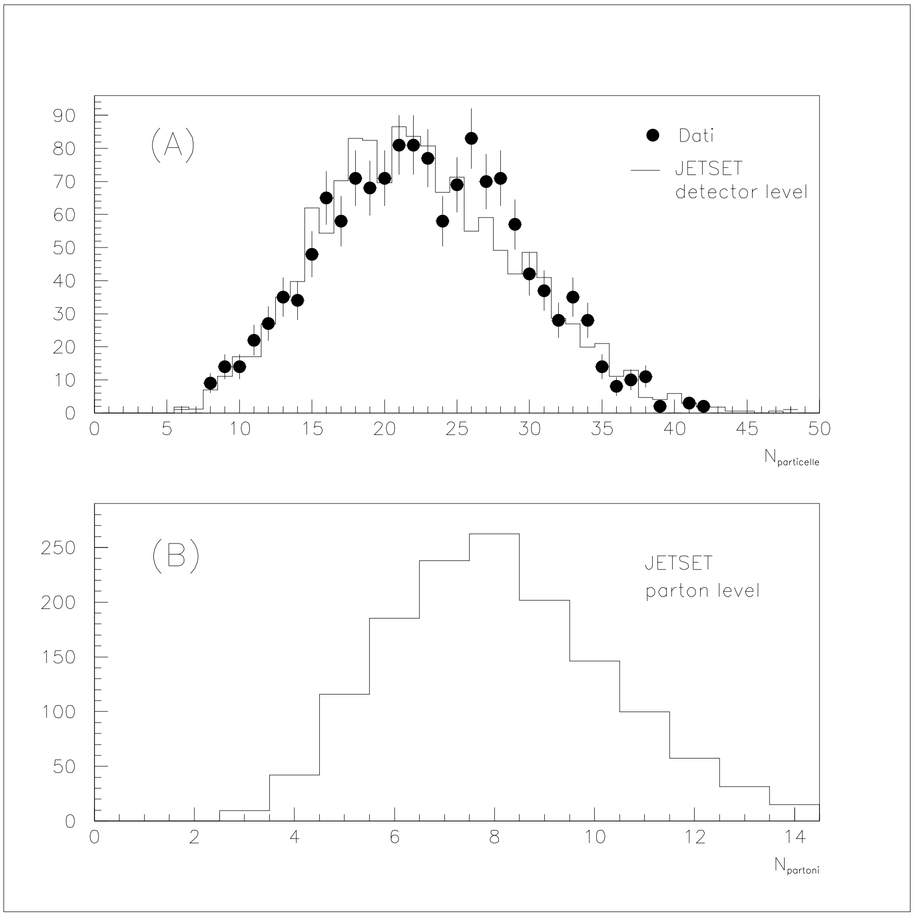

Figure 8: *(A) Multiplicity of hadronic events with an isolated shower in data and in simulation. (B) Multiplicity of the partonic level of JETSET in hadronic events with FSR photon.*

The conversion factors c_1 and c_2 for $\sigma^{tot}_{q\bar{q}\gamma}$ and for $\mathcal{R}_3$, computed for $y_{cut} = 0.02$ are reported in Table 3. They will be used to extract $\alpha_s^{(1)}$ and the normalization factor $\mathcal{N}$ from the data.
Having $c_2(\sigma^{tot}) > 1$ does not mean that in DELPHI the efficiency for hadronic events with final state photon radiation is greather than 1! In fact, the isolation cuts are not the same at the hadron and at the detector level. At the hadron level one must require to have no energy at all in the isolation cone, in analogy with ME generation which does not allow for it. On the contrary, at the detector level the apparatus sensitivity requires that some small amount of energy, here 500 MeV, would be admitted inside the cone.

7 Comparison with GNJETS and EEPRAD

Having all the conversion and correction factors, one is ready to compare DELPHI data with the ME predictions.
The comparisons of the experimental n-jet rates as a function of y_{cut} with the ones computed using the two MC programs are shown in Fig. 10 and 11. The width of the ME predictions accounts for the variation of the parameters described in section 2 and from the variation of $\alpha_s^{(1)}$ from 0.143 and 0.197 in GNJETS and from 0.142 to 0.204 in EEPRAD, as will be justified soon.

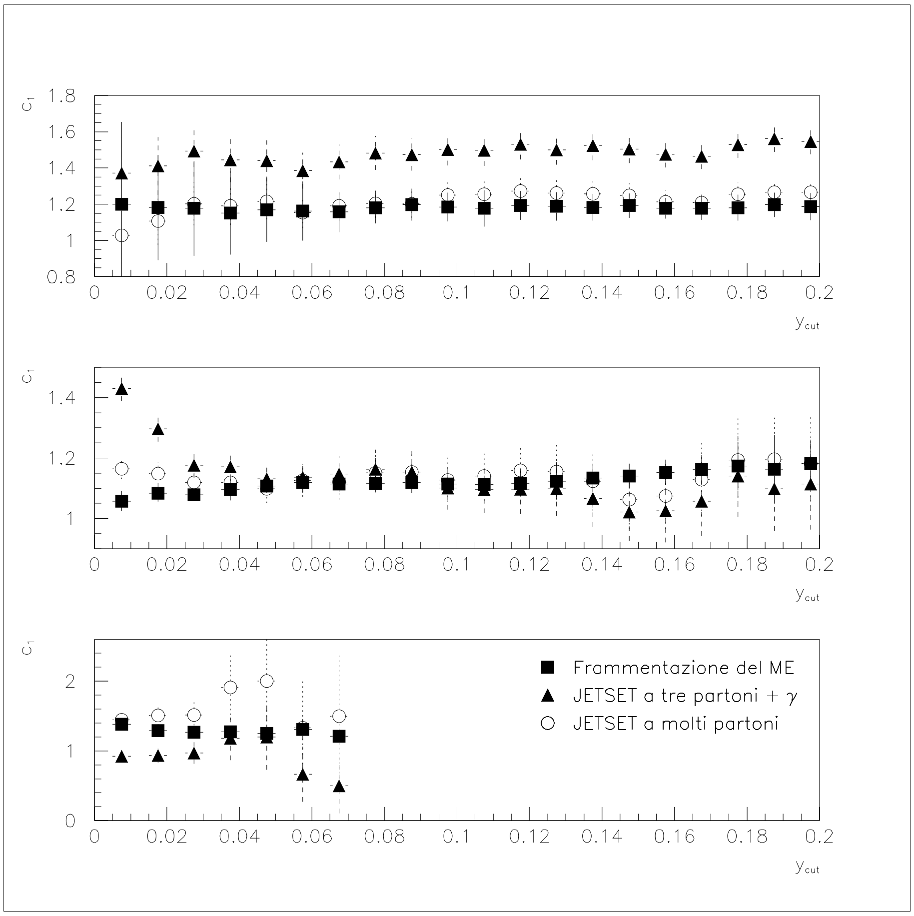

Figure 9: *Corretion factors c_1 computed using the ME fragmentation (squares) compared with the ones got from the parton level of JETSET with many (circles) or only 3 partons apart from the photon (triangles) for* 1, 2 *and* 3 *jets events plus* γ

In order to extract the MC free parameters, when working at $y_{cut} = 0.02$ one gets the best compromise between data statistics and independence from the variation of ME generation parameters. The ratio $\mathcal{R}_3$ at $y_{cut} = 0.02$ is

$$\mathcal{R}_3(y_{cut} = 0.02) = 0.100 \pm 0.015 \pm 0.010 \tag{36}$$

where the first error is statistical (binomial) and the second one comes from the selection of the FSR showers.
Comparing that ratio with the corresponding ratios in GNJETS and EEPRAD one gets:

$$\alpha_s^{(1)} = 0.170 \pm 0.027 \pm 0.008 \qquad (GNJETS) \tag{37}$$

$$\alpha_s^{(1)} = 0.173 \pm 0.031 \pm 0.008 \qquad (EEPRAD) \quad . \tag{38}$$

The different contributions to the errors are listed in Table 4. Since $\mathcal{R}_3$ is a relative jet ratio, most of the errors that enter in the normalization cancel and the main contribution remains the one coming from the sample statistics.
The normalization factor is extracted taking into account the error on $\alpha_s^{(1)}$, by adding its variation to the theoretical ME uncertainties, as was already done in Fig. 10 and 11. Comparing the inclusive

	c_1	c_2
σ_{tot}	1.11 ± 0.03	0.88 ± 0.03
$\mathcal{R}_3$	1.17 ± 0.05	1.07 ± 0.13

Table 3: c_1 = *(parton level) / (hadron level) and* c_2 = *(hadron level) / (detector level) correction factors used to extract the free parameters from MC's at* $y_{cut} = 0.02$

	GNJETS	EEPRAD
Statistics	0.022	0.025
Composition	0.013	0.016
Error on c_2	0.010	0.011
Tot. experimental	0.027	0.031
Error on c_1	0.008	0.008
Theor. error on ME	0.004	0.002
Tot. theoretical	0.008	0.008

Table 4: *Experimental and theoretical components of the errors on* $\alpha_s^{(1)}$ *when comparing data with GNJETS and EEPRAD at* $y_{cut} = 0.02$

$q\bar{q}\gamma$ cross sections at $y_{cut} = 0.02$ one gets:

$$8c_u + 3c_d = 12.3 \pm 1.3 \pm 0.6 \qquad (GNJETS) \tag{39}$$

$$8c_u + 3c_d = 11.8 \pm 1.2 \pm 0.5 \qquad (EEPRAD) \quad . \tag{40}$$

The different contributions to the errors are shown in Table 5. The main contribution to the uncertainty comes from the determination of the number of FSR given by equation 34.
One should underline that, using the method proposed in this work, the error coming from composition is almost purely a statistical one. Avoiding to use the hard to model lateral shower development in the HPC simulation, the error on the sample composition depends only on signal and reference samples statistics and can be reduced by analysing more data. On the contrary, an uncertainty coming from MC is irreducible and would affect more and more the precision of the results as the number of collected data increases.

7.1 c_u and c_d from the normalization

In the ME calculations the quarks are assumed to be massless. Such an approximation is correct, at the LEP energies, for what the lighter quarks are concerned. It is not obvious that the same holds for the 5.2 GeV b quark.
The effect of the quark masses should consist in reducing the phase space available for photon radiation, thus decreasing the FSR ratio.

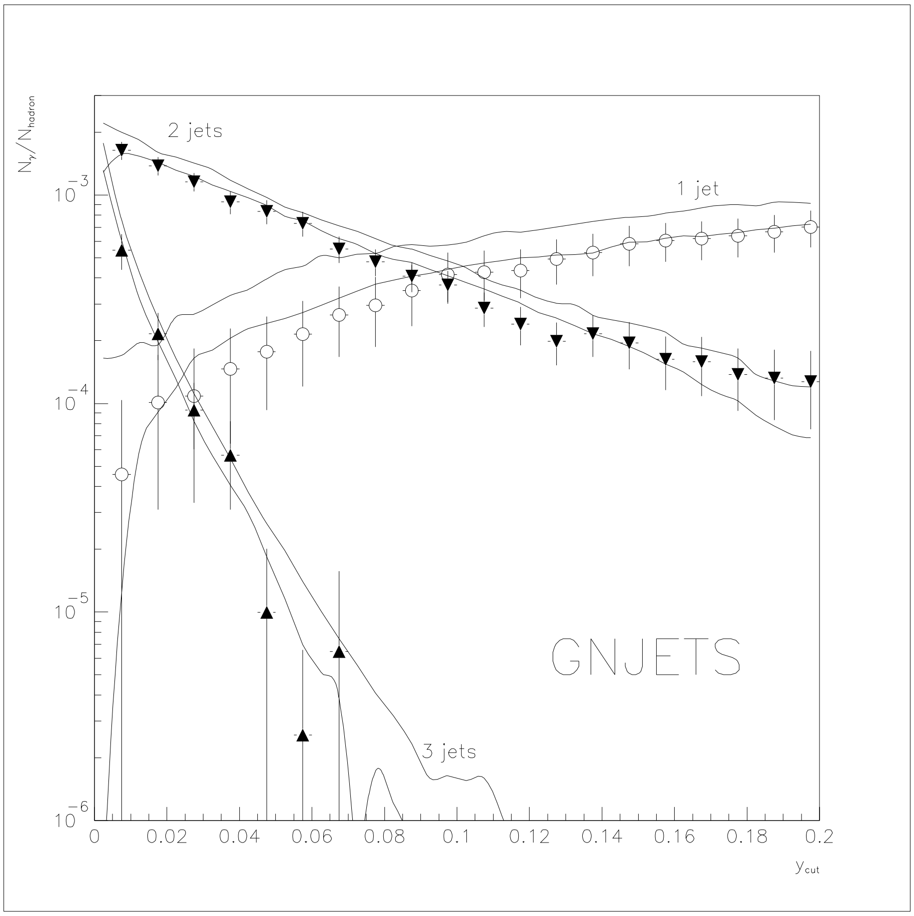

Figure 10: *Comparison of the cross sections for* 1, 2 *and* 3 *jets events between 1992 DELPHI data (points with errors) and GNJETS (strips representing the mean value plus and minus* 1σ*). In all cases the associated errors combine the statistical and the systematic ones. Points at different* y_{cut} *are strictly correlated.*

The effect of the b quark mass has been studied in [25], using a photon energy cut that is similar to the one used in the present analysis. As a result of this study, they suggest that the non zero b mass can be taken into account changing the expression $(8c_u + 3c_d)$ in the normalization factor with $(8c_u + (2+\epsilon)\, c_d)$, where $\epsilon = (0.8 \pm 0.1)$. The previous expression will be used to derive the *up* and *down* type quarks couplings to the Z^0.
From 39, 40 and 10 one gets:

$$c_u = \quad 0.99 \pm 0.23 \tag{41}$$
$$c_d = \quad 1.58 \pm 0.15 \quad , \tag{42}$$

comparing DELPHI data with GNJETS, and

$$c_u = \quad 0.90 \pm 0.21 \tag{43}$$
$$c_d = \quad 1.63 \pm 0.14 \quad , \tag{44}$$

comparing DELPHI data with EEPRAD.

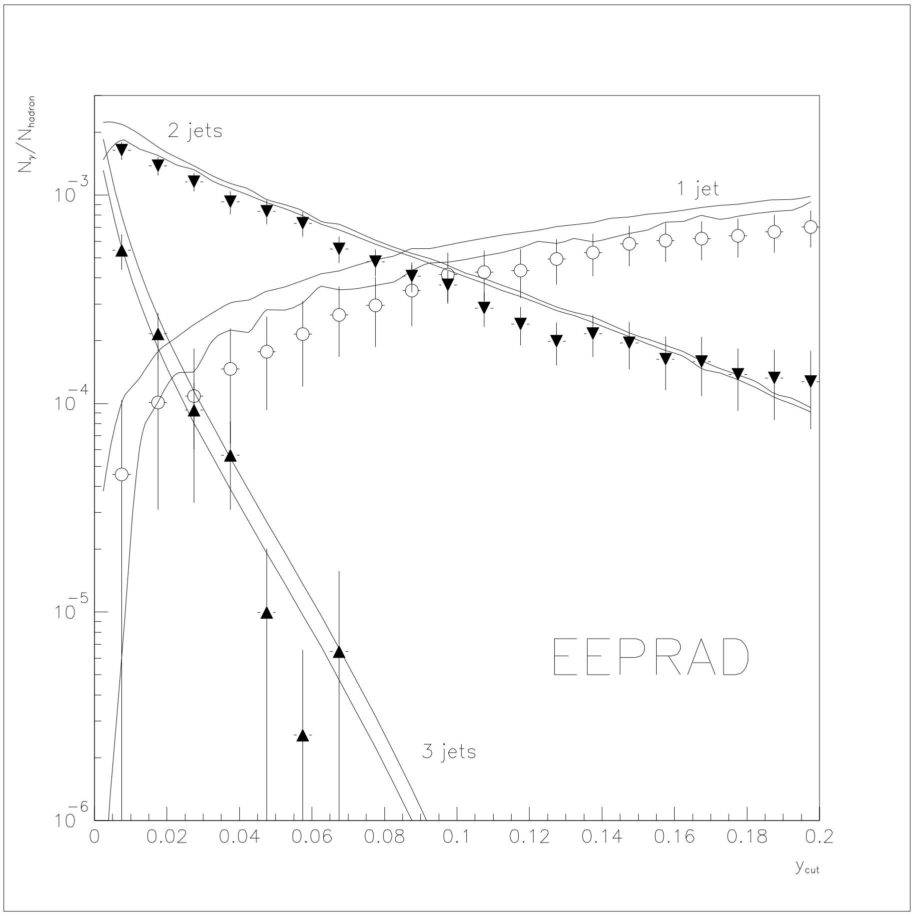

Figure 11: *Comparison of the cross sections for* 1, 2 *and* 3 *jets events between 1992 DELPHI data (points with errors) and EEPRAD (strips representing the mean value plus and minus* 1σ*). In all cases the associated errors combine the statistical and the systematic ones. Points at different* y_{cut} *are strictly correlated.*

The intersections of the two linear combinations of c_u and c_d are compared with the SM point ($c_u(SM) = 1.145 \pm 0.002$, $c_d(SM) = 1.477 \pm 0.001$) in Fig. 12 and 13.

8 Conclusions

A new method of selecting FSR photons in the hadronic decays of the Z^0 has been applied on DELPHI 1992 data. The results found are already comparable with those obtained applying more traditional methods; they are expected to improve with the available statistics. Indeed the amount of irreducible systematic uncertainties arising from modelization is kept very low and the "experimental systematics" on the measurements will scale with statistics.
From a comparison of the experimental FSR rates with two ME calculations at $\mathcal{O}(\alpha\alpha_s)$, the free parameters of the calculations have been derived.
Comparing with GNJETS one has:

$$\alpha_s^{(1)} = 0.170 \pm 0.27 \pm 0.08$$

	GNJETS	EEPRAD
Statistics	0.56	0.54
Composition	1.07	1.03
ISR	0.08	0.08
$\tau^+\tau^-$	0.03	0.03
ΔE	0.11	0.10
Extrap. to 4π	0.10	0.09
Error on c_2	0.33	0.32
Tot. Experimental	1.27	1.21
ME Statistics	0.35	0.20
Var. parameters	0.28	0.12
Var. $\alpha_s^{(1)}$	0.31	0.35
Error on c_1	0.32	0.31
Tot. theoretical	0.62	0.52

Table 5: *Experimental and theoretical components of the error on normalization when comparing data with GNJETS and EEPRAD at* $y_{cut} = 0.02$

$$\mathcal{N} = 12.3 \pm 1.3 \pm 0.6\,.$$

Comparing with EEPRAD:

$$\begin{aligned} \alpha_s^{(1)} &= 0.173 \pm 0.31 \pm 0.08 \\ \mathcal{N} &= 11.8 \pm 1.2 \pm 0.5\,. \end{aligned}$$

$\mathcal{N}$ represents $8c_u + 3c_d$ in a massless quark theory. Taking into account the b quark mass, the contribution of the *down* type quarks is slightly suppressed. The u and d quarks couplings to the Z^0 are derived to be:

$$\begin{aligned} c_u &= \quad 0.99 \pm 0.23 \\ c_d &= \quad 1.58 \pm 0.15 \end{aligned}$$

from the comparison with GNJETS, and

$$\begin{aligned} c_u &= \quad 0.90 \pm 0.21 \\ c_d &= \quad 1.63 \pm 0.14 \end{aligned}$$

from the comparison with EEPRAD.
Comparing these numbers with SM predictions

$$\begin{aligned} c_u(SM) &= \quad 1.145 \pm 0.002 \\ c_d(SM) &= \quad 1.477 \pm 0.001 \end{aligned}$$

one can see that there is agreement within about one standard deviation.
Nevertheless, taking into account the measurements of the other LEP experiments ([24], [25], [26]), it is clear that all the experiments agree very well among each other, all sitting around 1σ below

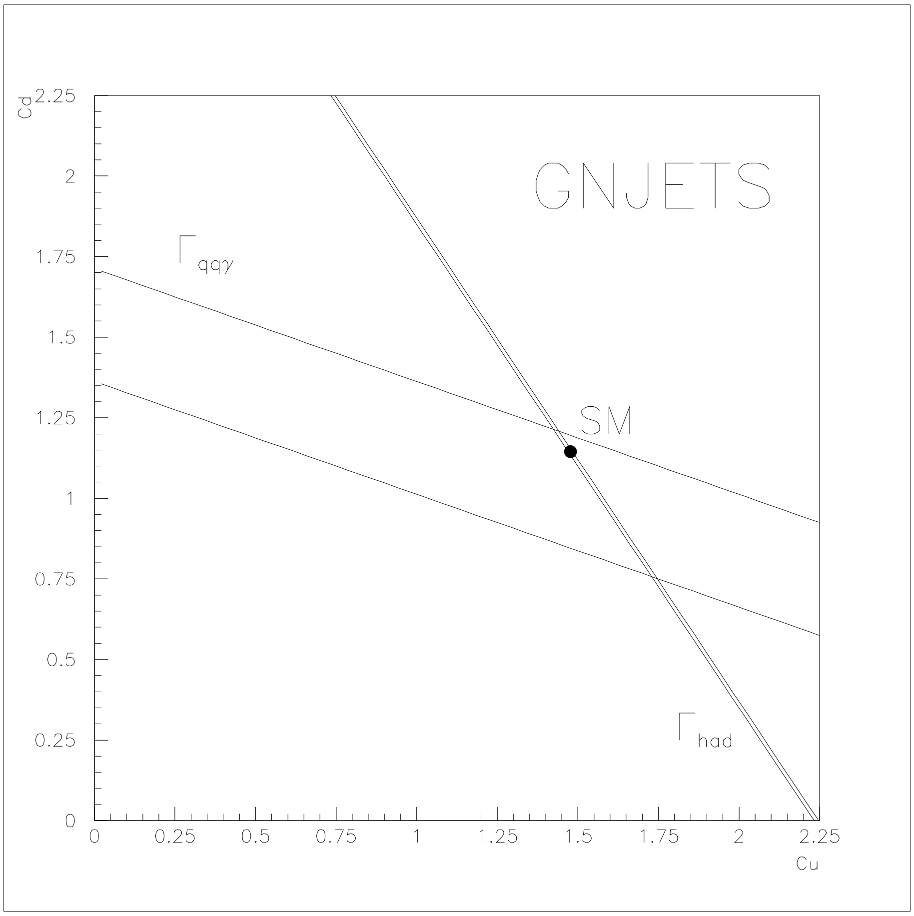

Figure 12: *c_u and c_d from the comparison of DELPHI 1992 data with GNJETS*

SM predictions for the overall FSR rate. There is a strong hint that, after combining all the results, the SM point would lie more significantly away from the LEP combined experimental point.
Such a discrepancy could come from the $\mathcal{O}(\alpha\alpha_s)$ calculations. A first order approximation in the strong coupling constant could be too crude, especially since $\alpha_s^{(1)}$ is estimated to be around 0.17, which is not such a small number...

9 Acknowledgments

I'm greatly indebted to Alberto Benvenuti, Alberto Demin, Michael Feindt, Alex Firestone, Francesco Navarria and Hubert Spiesberger for useful discussions and suggestions during the various stages of this work.

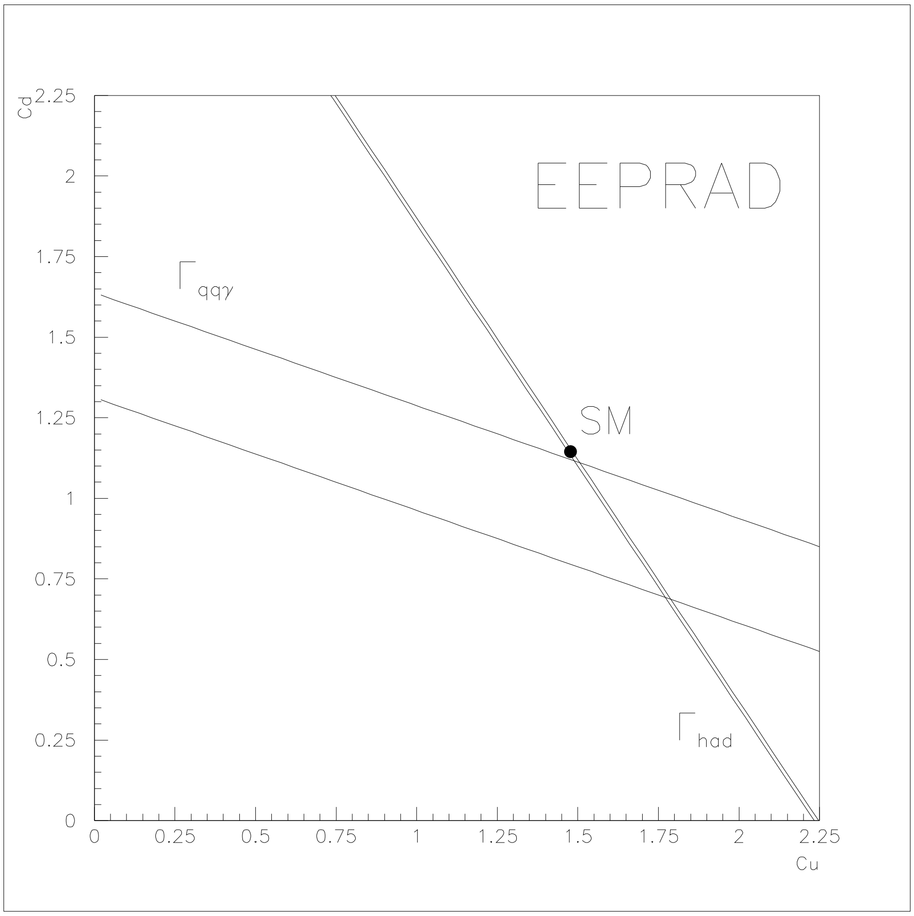

Figure 13: c_u *and* c_d *from the comparison of DELPHI 1992 data with EEPRAD*

References

[1] P. Mättig and W. Zeuner, Zeitschr. Phys. **C52** (1991) 31;
F.A. Berends, R. Kleiss, S. Jadach, Nucl. Phys. **B202** (1982) 63;
E. Laermann, et al., Nucl. Phys. **B207** (1982) 205.

[2] P. Abreu, et al., (DELPHI Collaboration) Z. Phys. **C53** (1992) 555.

[3] P. Mättig, H. Spiesberger and W. Zeuner, CERN-PPE/93-119.

[4] G. Kramer and H. Spiesberger, in *Proceedings of the Workshop on Photon Radiation from Quarks*, Annecy France, 2-3 Dec. 1991, Ed. S. Cartwright, CERN 92-04, p. 26; DESY preprint 92-022 (1992).

[5] G. Kramer and B. Lampe, Phys. Lett. **B269** (1991) 401.

[6] E. W. N. Glover and W. J. Stirling, Phys. Lett. **B295** (1992) 128.

[7] Yu.L. Dokshitzer, *contribution to the Workshop on Jets at LEP and HERA, Durham, dec. 1990.*

[8] Z. Kunszt e P. Nason, in *Z Physics at LEP1*. CERN-89-08, Vol. 1.

[9] Particle Data Group, Phys. Rev. **D45** (1992), Part 2.

[10] The LEP Collaborations (ALEPH, DELPHI, L3, OPAL) and the LEP Electroweak Working Group, CERN-PPE/93-157.

[11] P. Abreu, et al. (DELPHI collaboration), CERN-PPE/94-08

[12] P. Aarnio, et al. (DELPHI Collaboration) Nucl. Instr. and Meth. **A303** (1991) 233.

[13] H.G. Fischer, Nucl. Instr. and Meth., **A265** (1988) 218;
A. Cattai, et al., Nucl. Instr. and Meth., **A235** (1985) 310;
H.G. Fischer and O. Ullaland, IEEE Trans. Nucl. Sci., **NS-27** (1980) 38.

[14] DELPHI Collaboration, DELPHI 89-44 PROG 137.

[15] DELPHI 91-22 PROG 161 Rev.

[16] M. Feindt, O. Podobrin, S. Schael, *PXPHOT, DELPHI note in preparation.*

[17] DELPHI Collaboration, DELPHI 87-96 PROG 99;
DELPHI Collaboration, DELPHI 87-97 PROG 100.

[18] A. Firestone, DELPHI 91-111 CAL 83.

[19] A. Firestone, et al., DELPHI 91-39 PROG 174.

[20] A. Perrotta, DELPHI 93-121 PHYS 339.

[21] R. Brandelik, et al. (TASSO Collaboration), Phys. Lett. **114B** (1982) 65.

[22] T. Sjöstrand, Comp. Phys. Comm. **27** (1982) 243;
T. Sjöstrand, Comp. Phys. Comm. **28** (1983) 229;
T. Sjöstrand, Comp. Phys. Comm. **39** (1986) 347;
T. Sjöstrand and M. Bengtsson, Comp. Phys. Comm. **43** (1987) 367;
T. Sjöstrand, CERN-TH 6488/92, May 1992, Revised Sept. 1992.

[23] H. Furstenau, DELPHI 93-17/PHYS 265

[24] D. Decamp, et al., (ALEPH Collaboration) Phys. Lett. **264B** (1991) 476;
D. Buskulic, et al., (ALEPH Collaboration) Z. Phys. **C57** (1993) 17.

[25] O. Adriani, et al., (L3 Collaboration) Phys. Lett. **292B** (1992) 472;
O. Adriani, et al., (L3 Collaboration) Phys. Lett. **301B** (1993) 136.

[26] M. Z. Akrawy, et al., (OPAL Collaboration) Phys. Lett. **246B** (1990) 285;
G. Alexander, et al., (OPAL Collaboration) Phys. Lett. **264B** (1991) 219;
P. D. Acton, et al., (OPAL Collaboration) Z. Phys. **C54** (1992) 193;
P. D. Acton, et al., (OPAL Collaboration) Z. Phys. **C58** (1993) 405.